Transactions of the Materials Research Society of Japan 29[4] 1385-1388 (2004)

$YBa_2Cu_3O_{7-d}$ Films with a Nanoparticulate Dispersion of Y_2BaCuO_5 for Enhanced Flux Pinning

Paul N. Barnes, Timothy J. Haugan, Michael D. Sumption,* Srinivas Sathiraju, Julianna M. Evans, and Justin C. Tolliver
Propulsion Directorate, Air Force Research Laboratory, WPAFB, Ohio 45433 USA
Fax: 81-937-656-4095, e-mail: paul.barnes@wpafb.af.mil
*Department of Materials Science and Engineering, The Ohio State University, Columbus, Ohio 43210 USA
Fax: 81-614-688-3677, e-mail: mdsumption+@osu.edu

A comparison study of $YBa_2Cu_3O_{7-x}$ (Y123) films incorporating a nano-particulate dispersion of second-phase Y_2BaCuO_5 (Y211) and Y123 films incorporating a material (X, not specified) more closely lattice matched with Y123 is given. The inclusion of the nano-particulate dispersion was for the purpose of increasing superconducting film's magnetic pinning strength with the resultant improved in-field critical current density. The Y211 particulate and X layered inclusions in the Y123 was accomplished with multiple consecutive depositions by pulsed laser ablation of the respective targets on $LaAlO_3$ substrates. Results substantiate growth of the Y211 was caused by lattice mismatching with the Y123 achieving a Y211 particle size of ~ 10-20 nm in diameter and ~ 4 nm in height. The Y123 phase maintained excellent epitaxy with high in-plane orientation with both Y211 and X materials. With the Y211 additions, the critical current densities of the films increased 3 – 5 times at applied magnetic fields of 1.6 T from 30 to 77 K as compared to high quality Y123 films with no Y211 additions. The lattice matched material resulted in degraded currents in applied magnetic fields although self-field values were on par with plain Y123. This may imply a possible nullification of the intrinsic Y123 pinning mechanisms with the X material interlayers.
Key words: YBCO, Flux Pinning, Nanoparticulates, Y_2BaCuO_5

1. INTRODUCTION

$YBa_2Cu_3O_{7-d}$ (Y123 or YBCO) superconductors are being considered for a variety of applications because of the high critical transition temperature (T_c > 92K) and high critical current densities (J_c) in applied magnetic fields. In particular, YBCO coated conductors are being developed as flat tape geometry high temperature superconducting (HTS) wire to be used in power applications such as transformers, generators, motors, power transmission cables, etc. Even though YBCO has good in-field properties, it is of interest to further enhance its performance by improving the flux pinning characteristics of the superconductor, especially since J_c rapidly declines in magnetic field applied in the c-axis direction. [1-2] An increase of the critical current in the superconducting film can lead to a higher engineering current density for the HTS wire, the more critical wire parameter. [3]

The mechanisms of flux pinning occurring in YBCO films grown on varying substrates (or buffered substrates) is not immediately evident since the coherence length in this superconductor is quite small, ξ ~ 1.5 – 2 nm. [4] Because of the small coherence length, a variety of atomic size structures or defects in the film can pin the fluxons. However, this does suggest that a high density of nano-sized particulates dispersed throughout the super-conductor can be an effective pinning structure.

Y_2BaCuO_5 (Y211) has previously been used to confer pinning in bulk YBCO superconductors, but this has been principally in melt textured and bulk material. [5-9] In these cases, the size of the Y211 inclusions were typically on the order of a micron in size and particle density was low resulting in mediocre pinning at best. If an effective way of introducing Y211 into Y123 can be devised, Y211 has several advantages to be used as a material for the incorporation of pinning centers into Y123. Y211 is chemically stable with Y123 resulting in little if any chemical diffusion or reaction. [10] Also, deposition conditions for Y211 growth are quite similar to Y123.

Recently, a method has been reported by T. J. Haugan et al. to incorporate Y211 sites into Y123 as a nano-particulate dispersion using pulsed laser deposition. [11] Alternating depositions of Y211 and Y123 were performed in very short intervals to accomplish this. Due to the lattice mismatch between Y211 and Y123, the Y211 formed islands of several nanometers in size during growth. A subsequent deposition of the Y123 on top of the Y211 particles dispersed on the Y123 layer resulted in epitaxial growth of the Y123 on the exposed parts of the Y123 surface. The process was continuously repeated to provide the desired thickness of the composite film. This paper uses the same procedure described in that report to compare to a lattice matched material to be used in lieu of the Y211. Comparison of the two resultant composite structures will be given.

2. EXPERIMENTAL PROCEDURE

The alternate layers of the Y211 nanoparticulate and the Y123 were deposited by pulsed laser deposition (PLD) using conditions reported previously. [11] Composite material was also produced using a substance (X), not specified, that is closely lattice matched with the Y123. The PLD conditions being similar to Y123 growth, but different. The laser ablation targets used were purchased commercially. The sequential PLD depositions were automated with the laser pulses trigger-actuated by computer control. Film growth was stopped between each layer for a period of about 12 seconds, while the other target was rotated into position.

A Lambda Physik laser, model LPX 305i, was used operating at the KrF wavelength of 248 nm. The laser fluence was ~ 3.2 J/cm^2 and the ablation spot size was ~ 1 x 6.5 mm^2 pulsing at the rate of 4 Hz. The oxygen deposition pressure was 300 mTorr as measured with a capacitance manometer. Pressure in the chamber was kept constant while the oxygen gas (99.999% purity) flowed in during growth at a rate of ~ 1 l/min. The targets were resurfaced periodically with sandpaper, and conditioned prior to any film deposition with ~ 80 pulses. The targets were rotated and rastered radially during deposition for uniform target wear.

Single crystal substrates were ultrasonically cleaned for 2 minutes each using first acetone, followed by dehydrated ethyl alcohol or isopropyl alcohol. Crystalline substrates of $SrTiO_3$ were used and were previously polished on the surface by the manufacturer. A thin layer of colloidal Ag paint was used to attach samples to the heater. Substrates sizes were approximately 3.2 x 3.2 mm^2.

After deposition, films were cooled from 785 °C to 750 °C at 1270 °C/hr before turning off the vacuum pumps and O_2 pressure control. Subsequently the O_2 flow was increased to ~ 1.5 l/min into the chamber. The films were then cooled from 750 °C to 500 °C at a rate of 1270 °C/h, and held at 500 °C for 30 minutes, during which the O_2 pressure reached 1 atm. The films were cooled from 500 °C to 250 °C at about 1250 °C/h, and from 250 °C to room temperature using the natural cooling rate of the heater block (~ 800 °C/h).

The bulk of the current density measurements are a magnetic J_c of the samples acquired by a vibrating sample magnetometer (VSM). Two systems were used: one at Ohio State University (0 to 2 T) and one on-site (0 to 9 T), a VSM attachment to the Quantum Design physical properties measurement system. A ramp rate from 11,400 A/m to 55,700 A/m was used. The J_c of the samples was estimated using a simplified Bean model, $J_c = 15 \cdot \Delta M/R$, where M is magnetization/volume from the M-H loops, and R is the radius of volume interaction (= square sample side) for consistency. [12] The film thickness and dimensions of each sample were measured multiple times to reduce errors of superconducting volume and R to < 5 %.

Transport current densities were acquired by the 4-point contact method using pogo pins for current contacts and a 1 μv/cm criterion. On these samples, the current and voltage contacts for the resistive measurement were patterned onto the films by DC magnetron sputter deposition of Ag with ~ 3 μm thickness. The contact resistance of the Ag capped different films was reduced by annealing in pure O_2 at 55O °C for 30 minutes, followed by annealing at 500 °C for (0.5-2) hrs, with heating and cooling rates of 200 °C/h.

The superconducting transition temperature (T_c) was measured using an AC susceptibility technique with the amplitude of the magnetic sensing field varied from 0.025 Oe to 2.2 Oe, at a frequency of approximately 4 kHz. The T_c measurements were accurate within $\leq$ 0.1 K at three calibration points: liquid He at 4.2 K, liquid N_2 at 77.2 K, and room temperature. X-ray diffraction θ-2θ scans were made with a Rigaku diffractometer, with a 2θ step-size of 0.03 Å and a count time of 1.8 s.

3. RESULTS AND DISCUSSION

The two particular composite samples used for direct comparison in this study are a ($Y211_{1.3nm}/Y123_{12.5nm}$) x 24 composite film and a ($X_{0.8nm}/Y123_{11nm}$) x 24 composite film, where the subscripts refer to the extrapolated thickness of the designated layer if it was continuous and flat and the times by designation being the total number of layers. Additional samples were also created in this study with the chosen samples being representative of the composite group. A variety of "thicknesses" of Y211 and Y123 were used for the (Y211/Y123) x N films, although only one set of "thicknesses" was used for the batch of (X/Y123) x N composite films.

The composite films generally displayed a sharp transition at T_c, as sharp as the plainY123 films, indicating good quality. See Fig. 1 for a Y211/Y123 composite film. Even so, a slight depression of T_c occurred for the composite films of less than 2 degrees. Transport measurement of the self-field J_c, at 77 K, indicated that the comparison composite films used in this study were both over 1 MA/cm^2.

Although transport J_c measurements at 77 K, self-field, indicated similar behavior, they were radically different in applied magnetic fields. Both the magnetic J_c in applied fields and transport J_c in applied fields substantiate the opposing behavior. See Fig. 2 for the ($Y211_{1.3nm}/Y123_{12.5nm}$) x 24 and the ($X_{0.8nm}/Y123_{11nm}$) x 24 composite film comparison. As in previous studies the (Y211/Y123) x N films all enhanced J_c, some significantly and some very little depending on the particular parameters used. However the J_c of the (X/Y123) x N samples rapidly degraded with increasing field.

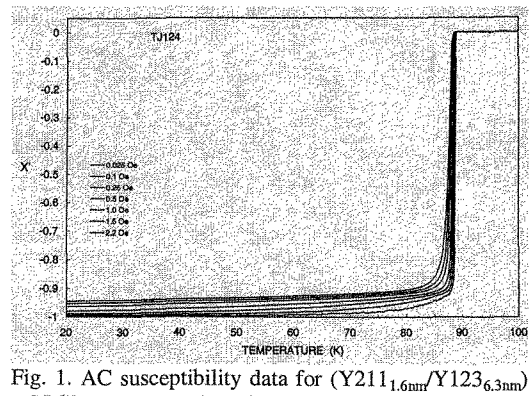

Fig. 1. AC susceptibility data for ($Y211_{1.6nm}/Y123_{6.3nm}$) x 35 film representative of most composite films.

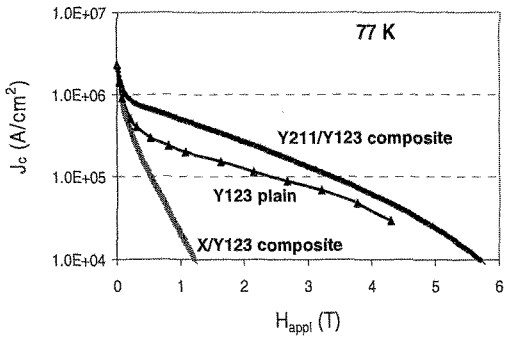

Fig. 2. In-field comparison of J_c, A) upper thick black data is $(Y211_{1.3nm}/Y123_{12.5nm})$ x 24 composite film, B) lower thick gray data $(X_{0.8nm}/Y123_{11nm})$ x 24 composite film, and C) a plain Y123 sample of good quality.

Differences in the two composite films are made clear by TEM. Fig. 3 is a TEM of the planar view of the prepared (Y211/Y123) x N composite film. The TEM bright-field micrograph of the film through planar view reveals the particle-like nature of defects throughout the material. Moiré fringelike patterns are seen due to the stress created by the inserted Y211 particles. Additional SEM and TEM not shown reveal the size of particles observed to be between 10 and 15 nm. The particle density is estimated to be ~ 10^{11} cm^{-2}.

Fig. 4 is a TEM that displays the layered structure of the (X/Y123) x N composite film in which the material X is closely lattice matched with Y123. The micrograph demonstrates that the (X/Y123) x N films are more of a multilayer structure as opposed to the (Y211/Y123) x N composite films which as more of a nano-particulate dispersion of Y211 in Y123. The structure is apparently the primary difference which results in the opposite behavior of the films. The (Y211/Y123) x N composite films improve J_c in applied magnetic fields over plain Y123, whereas the thin inter-layers of substance X in the composite films degrades the performance of Y123 when placed in a magnetic field.

The difference in growth of the inserted material (either Y211 or X) during deposition is evidently directed related to the lattice matching parameters of the material. For Y211, the material is mismatched by 2-9 % resulting in island growth. For substance X, which more closely matches the lattice parameter of the Y123, uniform growth occurs as oppose to island growth.

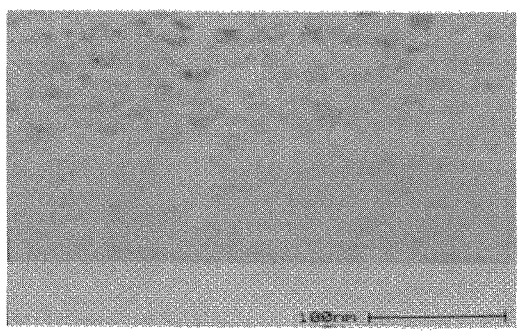

Fig. 3. TEM bright field of (Y211/Y123) x N film through planar view.

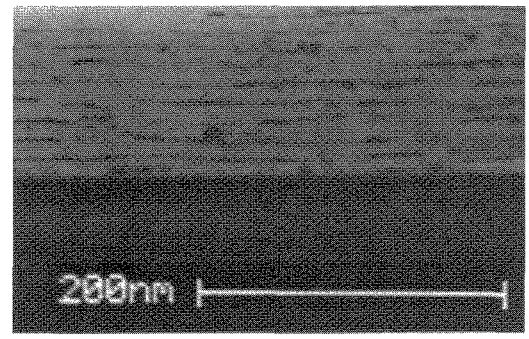

Fig. 4. TEM cross-section of the (X/Y123) x N composite film. The micrograph indicates that the (X/Y123) x N films are more like a multilayer film as opposed to the (Y211/Y123) x N composite films which are a nano-particulate dispersion of Y211 in Y123.

A final result of the composite films is the smoothness of the surface compared to Y123 films grown. Fig. 5 compares the surface of a one micron thick Y123 film with a one micron thick (Y211/Y123) x N composite film. The composite films remain smooth while the Y123 films tend to increase in surface roughness as they are grown thicker. This indicates the potential to grow thicker composite films without as much degradation of the current carrying characteristic of the sample due to poor morphology.

4. CONCLUSIONS

Using PLD, the island-growth mechanism of lattice-mismatched Y211 on Y123 achieved a surface particle density ~ 10^{11} cm^{-2} of Y211 nanoparticles. The (Y211/Y123) x N composite films grown by this approach resulted in a particulate dispersion of Y211 throughout the Y123 with excellent pinning properties. However, using a substance that is more closely lattice-matched with the Y123, a thin nanolayer structure resulted. With the Y211 addition, the critical current densities increased 3-5 times for applied magnetic fields of 1.6 T from 30 K to 77 K. In the (X/Y123) x N composite films a degradation from the expected performance of plain Y123 films occurs. Addition of Y211 had neglible effect on c-axis and ab in-plane orientation of the subsequent Y123 phase growth. Finally, the multi-growth deposition produces smooth film surfaces with reduced secondary particles that may allow thicker film growth without J_c degradation.

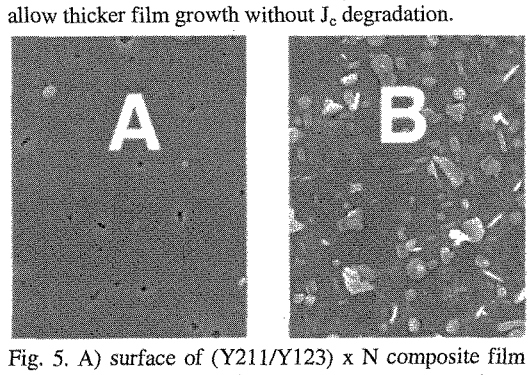

Fig. 5. A) surface of (Y211/Y123) x N composite film and B) surface of Y123 film. Both films are one micron thick.

[1] S. R. Foltyn, E J. Peterson, J. Y. Coulter, P. N. Arendt, Q. X. Jia, P. C. Dowden, M. P. Maley, X. D Wu and D. E. Peterson, *J. Mater. Res.*, **12**, 2941-2946 (1997).
[2] T. Aytug, M. Paranthaman, S. Sathyamurthy, B. W. Kang, D. B. Beach, E. D. Specht, D. F. Lee, R. Feenstra, A. Goyal, D. M. Kroeger, K. J. Leonard, P. M. Martin and D. K. Christen, "Reel-to-Reel Continous Chemical Solution Deposition of Epitaxial Gd_2O_3 Buffer Layers on Biaxial Textured for the Fabrication of $YBa_2Cu_3O_{7-d}$ Coated Conductors," *ORNL Superconducting Technology Program for Electric Power Systems, Annual Report for FY 2001*, ORNL/HTSPC-13, pp. 1-25 – 1-34.
[3] G. N. Riley, Q. Li and L. G. Fritzmeier, *Current Opinion in Solid State and Mat. Sci.*, **4**, 473-478 (1999).
[4] D. Larbalestier, A Gurevich, D. M. Feldmann and A. Polyanskii, *Nature*, **414**, 368-377 (2001).
[5] M. Murakami, S. Gotoh, H. Fujimoto, K. Yamaguchi, N. Koshizuka and S. Tanaka, *Supercond. Sci. Technol.*, **4**, S43 (1991).
[6] S. Jin, G. W. Kamlott, T. H. Tiefel, T. Kodas, T. L. Ward and D. M. Kroeger, *Physica C*, **181**, 57-62 (1992).
[7] D. Shi, S. Sengupta, J. S. Luo, C. Varanasi, and P. J. McGinn, *Physica C*, **213**, 179-184 (1993).
[8] M. Chopra, S.W. Chan, R. L. Meng and C. W. Chu, *J. Mater. Res.*, **11**, 1616 (1996).
[9] S. Sengupta, D. Shi, J. S. Luo, A. Buzdin, V. Gorin, V. R. Todt, C. Varanasi and P. J. McGinn, *J. Appl. Phys.*, **81**, 7396 (1997).
[10] Phase Diagrams for High Tc Superconductors, edited by J. D. Whitler and R. S. Roth, (American Ceramic Society, Westerville OH, 1991).
[11] T. J. Haugan,, P. N. Barnes, I. Maartense, E. J. Lee, M. D. Sumption and C. B. Cobb, *J. Mater. Res.*, **18**, (2003).
[12] J. R. Thompson, L. Krusin-Elbaum, Y. C. Kim, D. K. Christen, A. D. Marwick, R. Wheeler, C. Li, S. Patel, D. T. Shaw, P. Lisowski and J. Ullmann, *IEEE Trans Appl. Supercond.*, **5**, 1876 (1995).

(Received October 13, 2003; Accepted July 1, 2004)